WOOD RESEARCH doi.org/10.37763/wr.1336-4561/67.4.545557
e-ISSN 2729-8906
67(4): 2022 545-557 pp.

EVALUATION OF THE DECAY LEVELS OF WOODEN COMPONENTS IN ARCADE BUILDINGS IN THE ANCIENT TOWN CHIKAN VIA POLARIZED LIGHT, FLUORESCENCE AND FTIR SPECTRA

YAN YANG, XIAOQIAN ZHANG, QIAN XU, PEIYANG WANG, SHILONG JIANG,
YAN MIN, WENYE SUN, BIN LI, YULONG FAN
NANYANG INSTITUTE OF TECHNOLOGY
CHINA

SHUANG YANG
HENAN UNIVERSITY MINSHENG COLLEGE
CHINA

(RECEIVED DECEMBER 2021)

ABSTRACT

In order to classify the decay levels of Chinese fir (*Cunninghamia lanceolata*) wood components in arcade buildings in the ancient town Chikan and to provide basic data for future protection measures, the extent of decay of the samples was determined via polarized light, fluorescence, and Fourier-transform infrared spectroscopy. The results were as follows: *(1)* The total birefringence brightness of crystalline cellulose and the green fluorescence brightness of the lignins were reduced to different degrees in almost all samples. *(2)* The absorption peaks at 1731 cm^{-1} representing hemicellulose and at 891 cm^{-1} representing cellulose in all samples disappeared. The absorption peak heights at 1370 cm^{-1}, 1159 cm^{-1} and 1058 cm^{-1} which represents holocellulose, and at 1508 cm^{-1}, 1424 cm^{-1}, and 1262 cm^{-1} which represents lignin decreased to varying degrees. *(3)* From the analysis, the decay level of wooden components in arcade buildings was divided into three classes, i.e., Level I (severe decay), Level II (moderate decay), and Level III (mild decay).

KEYWORDS: Ancient town Chikan, Chinese fir (*Cunninghamia lanceolata*), wooden components, decay levels, polarized light, fluorescence, Fourier-transform infrared spectra.

INTRODUCTION

Chikan, is located in the economic development zone in the southwest of the Pearl River Delta in Guangdong Province, China. The uniform arcade buildings are one of the primary characteristics of Chikan, and also the primary building form of the local modern towns along the street.

Chikan town is located in the south of the Tropic of Cancer, a subtropical monsoon climate. The annual average temperature is 20-22°C, the highest temperature is 37.3°C, and the lowest temperature is 13.4°C. Moreover, there is more precipitation, mainly from April to September. Abundant precipitation makes the annual relative humidity of the environment being above 84.0%. The warm and rainy weather also created suitable conditions for the growth of decaying fungi.

However, some wooden components have been degraded to different degrees under environmental temperature and humidity changes, or microorganisms, insects, ultraviolet rays, etc., due to long-term exposure to air (Fig 1a). The macroscopic degradation behaviors usually inevitably happen with the super microscopic degradation of chemical components of the cell walls, including cellulose, hemicellulose, and lignins (Ferraz and Durán 1995, Arias et al. 2010, Bari et al. 2019, 2020, Girometta et al. 2020, Yang et al. 2020a,b). Cellulose acts in a framework role and hemicellulose acts in an interstitial filling role, while lignin provides a skeleton or framework in the cell wall with cellulose providing strength. The reduction of the chemical components then can decrease the physical and mechanical properties of wooden components, eventually affecting the safety and the life span of the Arcade buildings (Choi et al. 2006, Brischke et al. 2019, Chang et al. 2019, Gao et al. 2019, Li et al. 2019, Bari et al. 2020). Therefore, the content change analysis of the cellulose, hemicellulose, and lignins could evaluate and judge the degree and level of decay in the wood components.

Wood cell walls have birefringent due to the crystalline region formed by the orderly arrangement of cellulose. Therefore, the presence or absence of a cellulose crystalline region in a wood cell wall can be observed by a polarized light microscope, in order to qualitatively determine the degradation of the wood cellulose crystalline region (Kanbayashi and Miyafuji 2016, Cui et al. 2016b, Yang et al. 2020a). In addition, wood cell walls can produce spontaneous fluorescence due to the existence of phenolic substances, i.e., lignins. Therefore, the concentration of lignins can be determined by the strength and weakness of lignin autofluorescence (Cui et al. 2016a,b, Yang et al. 2020a,c).

In addition, the three primary chemical components of wood have corresponding Fourier-transform infrared spectroscopy (FTIR) absorption peaks. The shapes, positions, and intensities of the absorption peaks will change accompanied by the change in the chemical components (Pandey and Pitman 2003, Stark and Matuana 2004, Ibrahim et al. 2007, Stark and Matuana 2007, Pandey and Nagveni 2009, Li et al. 2010, Monrroy et al. 2011, Zeng et al. 2012, Tomak et al. 2013, Xu et al. 2013, Liu et al. 2017a, Tamburini et al. 2017, Croitoru et al. 2018, Fahey et al. 2019, Wentzel et al. 2019, Bari et al. 2020, Dong et al. 2020, Yang et al. 2020c). Therefore, the changes in the wood functional groups and the contents of the three primary

chemical components can be determined according to the changes in the absorption peak intensities.

These methods of polarized light, fluorescence, and FTIR spectra are helpful to evaluate the degradations of chemical components and have been increasingly applied to the analysis of the extent of decay of wooden components in ancient buildings because of the advantages of requiring a minimal number of samples and resulting in less damage to the ancient buildings (Cui et al. 2016b, Yang et al. 2020a,c).

The goals of this study were to gain the distribution and content of cellulose and lignins in wood components from Chikan observed with polarized light and fluorescence, respectively. In addition, this study aimed to determine the changes in the chemical components via FTIR analysis and to evaluate the decay levels of the wooden components. The results of this study would provide reliable data support and guidance for the reasonable protection and restoration of wooden components in Chikan in the future.

MATERIAL AND METHODS

Materials

Samples No. 1 through 10 were randomly collected from the decay wooden components in the roof systems in Chikan arcade buildings, Kaiping City, Jiangmen City, Guangdong Province, China (Fig. 1a), and were identified as Chinese fir (*Cunninghamia lanceolata*) (Taxodiaceae) (Fig. 2) (Cheng et al. 1992). The control sample was obtained from the new replaced wooden components in Chikan arcade buildings (Fig. 1b).

(a) Decayed wooden components. (b) Control sample. (c) The arcade buildings of Chikan.

Fig. 1: The samples in this study.

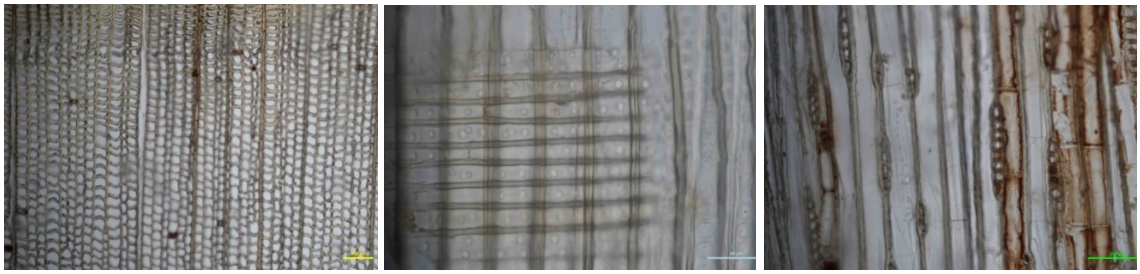

(a) Transverse section. (b) Radial section. (c) Tangential section.

Fig. 2: Microstructures of samples under a bright-field light.

Preparation of sections

The sections were made according to the following steps (Yang et al. 2020a,c, 2021a): *(1)* Sectioning: the samples were sectioned with a microtome (HistoCore AUTOCUT, Leica Biosystems, Wetzlar, Germany). The sections were approximately 10 μm to 15 μm thick and included the transverse, radial, and tangential sections. *(2)* Dehydration: the slices were dehydrated with a 50%, 75%, 95%, and 100% ethanol solution; each concentration treatment lasted for 10 min. *(3)* Defatting: the slices were defatted with dimethylbenzene solution for 3 min. *(4)* Sealing with neutral gum: neutral gum was used to seal the slices. To avoid the effect of dye on the polarized light and fluorescence, the sections used for observation via polarized light and fluorescence were not dyed with safflower O dye.

Preparation for Fourier-transform infrared spectroscopy (FTIR) analysis

Oven-dried wood powder which was processed using an agate mortar and spectrum potassium bromide (KBr) were fully mixed in a ratio of 1 to 150, respectively, poured into an agate mortar, and ground into a powdered form while keeping the wood powder and KBr in a dried condition by using a high-wattage lamp throughout the whole process. The powder mixture (approximately a few mg) was compressed into sliced samples using a powder tablet press machine (FW-5A, Uncommon Technology Development Co., China) for FTIR analysis (Yang et al. 2015, 2020b, 2021b).

Observations under bright-field, polarized light, and fluorescence

The deformation of the cell walls was analyzed under bright-field light; the distribution and content of the cellulose were analyzed under polarized light; and the distribution and content of the lignins were analyzed under fluorescence with a microscope (ECLIPSE Ni-U, Nikon, Tokyo, Japan) for the analysis of the decay levels of the wooden components (Cui et al. 2016b, Yang et al. 2020a,c).

Fourier-transform infrared spectroscopy (FTIR) testing

The FTIR spectra were generated using a FTIR spectrophotometer (ALPHA2, Bruker, Billerica, MA) at a range of 4000 cm^{-1} to 400 cm^{-1} to provide detailed information on the functional groups present in the sample surface (Yang et al. 2015, 2020b, 2021b). Scans were run at a resolution of 4 cm^{-1}, and the spectra was obtained using attenuated total reflectance. A minimum of five scans per specimen were operated to calculate their average. The ratio of the absorption peak height ratios of carbohydrates to lignins was used to characterize the contents of the chemical components. The absorption peak height was calculated according to literature (Pandey and Pitman 2003, Li et al. 2010, Xu et al. 2013, Bari et al. 2020, Dong et al. 2020, Yang et al. 2020b). The lignin content was characterized by the values of H 1508/I H1159 and H 1508/H 1058; the hemicellulose and cellulose contents were characterized by the values of H 1731/H 1508 and H 897/ H1508, respectively, while the holocellulose content was characterized by the values of H 1370/H 1508, H 1159/ H1508, and H 1058/H 1508.

RESULTS AND DISCUSSION

Polarized light and fluorescence analysis

Figs. 3-6 show that almost all of the cell walls of the tracheids in all samples remained basically intact except for part of the cell walls in the earlywood tracheids which were damaged in shape when viewed under a bright-field light (Fig. 3a).

Under polarized light, the distribution and content of the cellulose crystalline regions of the cell walls in wood can be qualitatively determined. In general, the higher the birefringence brightness is, the higher the cellulose content is (Cui et al. 2016b, Kanbayashi and Miyafuji 2016, Yang et al. 2020a). The birefringence of the crystalline cellulose in samples No. 1, 2, 3, 5, and 6 occurred in the cell wall corners (CC) and the compound middle lamellas (CML) of tracheids, and were almost lacking in secondary wall middle layers (S_2) and inner layers (S_3), especially in the radial walls. As such, the total birefringence brightness was reduced greatly (Fig. 3b), when compared with the control (Fig. 6b). Fungi do not usually enter CC in softwoods because of the existence of lots of guaiacyl lignins, which are resistant to decomposition in CC (Guo et al. 2010). Under the protection of guaiacyl lignins, fungi only eroded the cell walls of cell lumens but not from CC, which makes the cell walls thinner (Highley et al. 1987). While the birefringence of crystalline cellulose in samples No. 4, 8, and 9 obviously occurred in the CC, CML, S_2, and S_3 of the tracheids (Fig. 4b), but was reduced largely compared with the control (Fig. 6b), while samples No. 7 and 10 (Fig. 5b) were consistent with the birefringence brightness in the control (Fig. 6b).

Under fluorescence, the green fluorescence brightness can provide the distribution and content of lignins; the greater the green fluorescence brightness is, the higher the relative content of the lignins is (Ma et al. 2013, Cui et al. 2016a,b, Liu et al. 2017a,b, Kiyoto et al. 2018, Yang et al. 2020a,c). The green fluorescence of the tracheid cell walls in samples No. 1, 2, 3, 5, and 6 were also more obvious, but the green fluorescence tinged with a faint yellow and the brightness was considerably reduced (Fig. 3c) compared with the control (Fig. 6c). In addition, while the green fluorescence brightness was also considerably reduced in samples No. 4, 8, and 9 (Fig. 4c), the samples No. 7 and 10 (Fig. 5c) were consistent with the green fluorescence brightness in the control (Fig. 6c).

From the brightness of both the birefringence of crystalline cellulose and the green fluorescence of lignins, it can be concluded that not only the crystalline cellulose but also the lignins in the samples were attacked by decay fungi to varying degrees; the extent of decay in samples No. 1, 2, 3, 5, and 6 was the greatest, followed by samples No. 4, 8 and 9, with samples No. 7 and 10 having the least amount of decay. Cellulose plays a role in the skeleton of the cell wall structure, and a reduction of the cellulose content therefore brings about a reduction in tensile strength, compressive strength, and other properties of the wooden components. Lignins play the role of bonding, and a decrease in lignin content therefore brings about a decrease in the hardness of the wooden components.

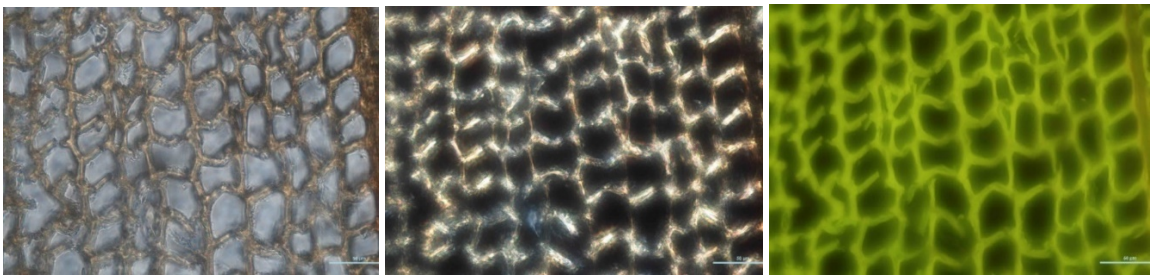

Level I (severe decay).
(a) Bright-field light. (b) Polarized light. (c) Fluorescence.

Fig. 3: Microstructures of the transverse sections in samples No. 1, 2, 3, 5, and 6.

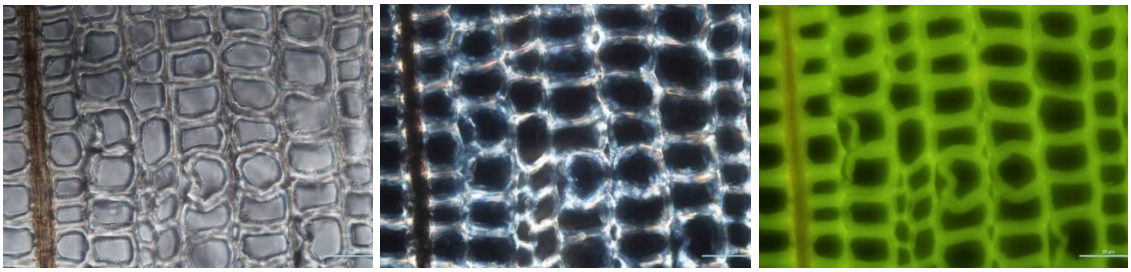

Level II (moderate decay).
(a) Bright-field light. (b) Polarized light. (c) Fluorescence.

Fig. 4: Microstructures of the transverse sections in samples No. 4, 8, and 9.

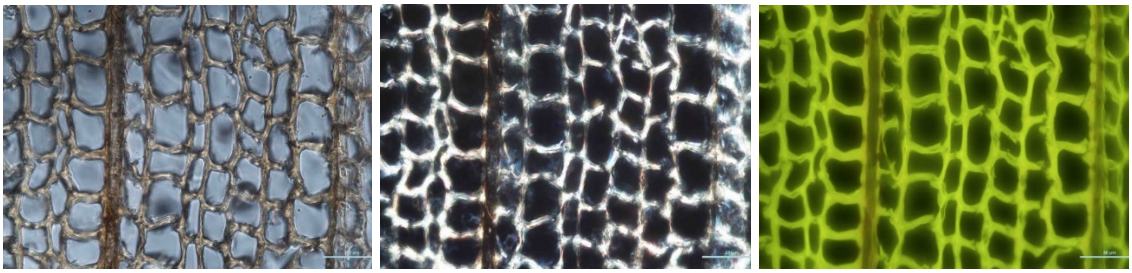

Level III (mild decay).
(a) Bright-field light. (b) Polarized light. (c) Fluorescence.

Fig. 5: Microstructures of the transverse sections in samples No. 7 and 10.

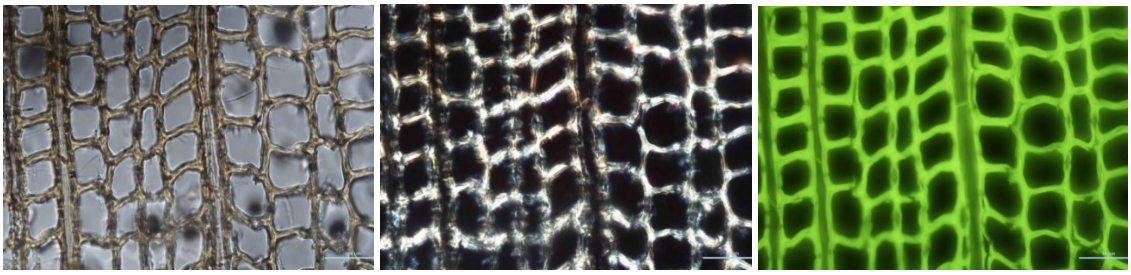

(a) Bright-field light. (b) Polarized light. (c) Fluorescence.

Fig. 6: Microstructures of the transverse sections in the control.

Fourier-transform infrared spectroscopy (FTIR) analysis

As shown in Figs. 7-9, the absorption peak positions of all samples in the region from 1800 cm^{-1} to 800 cm^{-1} had no displacement, but the intensities had obvious changes. Compared with the control, the absorption peaks at 1731 cm^{-1}, representing hemicellulose, at 891 cm^{-1},

representing cellulose, and at 1312 cm^{-1}, representing holocellulose, i.e., the sum of cellulose and hemicellulose, in all samples disappeared (Fig. 7-9).

In addition, the absorption peak intensities at 1370 cm^{-1}, 1159 cm^{-1}, and 1058 cm^{-1}, which represent holocellulose, disappeared or greatly decreased, while the absorption peak heights at 1370 cm^{-1} decreased by 100% (in samples No. 1, 2, 3, 5, and 6), 22% (in samples No. 4, 8, and 9) and 11% (in samples No. 7 and 10). The absorption peak at 1159 cm^{-1} decreased by 59%, 22%, and 3%, with respect to the previous sample groupings, and those at 1058 cm^{-1} decreased by 50%, 41%, and 5%, with respect to the previous sample groups (Tab. 1). From the results, it was concluded that the reduced degree of carbohydrate, which was degraded by decay fungi, was the greatest in samples No. 1, 2, 3, 5, and 6, followed by samples No. 4, No. 9, and No. 11, and was the least in samples No. 7 and 10.

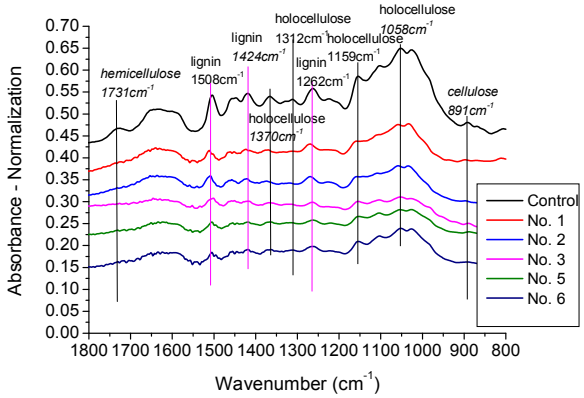

Level I (severe decay).

Fig. 7: Infrared spectrum of samples No. 1, 2, 3, 5, and 6.

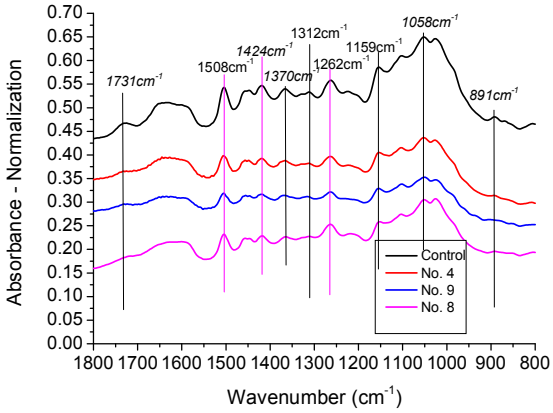

Level II (moderate decay).

Fig. 8: Infrared spectrum of samples No. 4, 8, and 9.

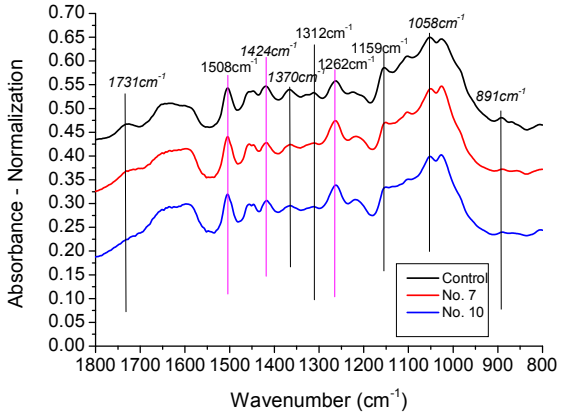

Level III (mild decay).

Fig. 9: Infrared spectrum of samples No. 7 and 10.

Tab. 1: The change rates of the absorption peak heights at different positions.

Decay levels	Samples	The absorption peak heights (cm^{-1})								
		1731	1508	1424	1370	1312	1262	1159	1058	897
	Control	0.023	0.062	0.026	0.018	0.011	0.030	0.037	0.022	0.013
Level I	No. 1, 2, 3, 5,	0	0.021	0.01	0	0	0.015	0.015	0.011	0

(severe decay)	and 6									
	Change amount	-100%	-66%	-62%	-100%	-100%	-50%	-59%	-50%	-100%
Level II (moderate decay)	No. 4, 9, and 11	0	0.038	0.017	0.014	0	0.025	0.029	0.013	0
	Change amount	-100%	-39%	-35%	-22%	-100%	-17%	-22%	-41%	-100%
Level III (mild decay)	No. 7 and 10	0	0.061	0.022	0.016	0	0.030	0.036	0.021	0
	Change amount	-100%	-2%	-15%	-11%	-100%	0%	-3%	-5%	-100%
Note: + - increase percentage, − - decrease percentage.										

Compared with the control, the absorption peak intensities at 1508 cm^{-1}, 1424 cm^{-1}, and 1262 cm^{-1}, which represent lignins, decreased considerably in all samples (as seen in Fig. 7 through Fig. 9). The absorption peak heights at 1508 cm^{-1} decreased by 66% (in samples No. 1, 2, 3, 5, and 6), 39% (in samples No. 4, 8, and 9), and 2% (in samples No. 7 and 10). The absorption peak at 1424 cm^{-1} decreased by 62%, 35% and 15%, with respect to the previous sample groupings; the absorption peak at 1262cm^{-1} decreased by 50%, 17% and 0%, respectively (as shown in Tab. 1). From the results, it was concluded that the reduced degree of lignins in samples No. 1, 2, 3, 5, and 6 was the greatest, followed by samples No. 4, 8, and 9, with no obvious reduction in samples No. 7 and 10. The decreasing trend of the lignins was the same as the trends in cellulose and hemicellulose.

Tab. 2 shows that the values of H 1508/H 1159 and H 1508/H 1058, representing the lignin contents in samples No. 1, 2, 3, 5, and 6, decreased from 1.68 to 1.40 and from 2.82 to 1.91, respectively, with 16% and 32% reductions, respectively. The decrease in the lignin contents showed a severe degradation of the lignins resulting from fungal decay. Meanwhile, the values of H 1731/H 1508, H 1370/H 1508, and H 897/H 1508, representing the carbohydrate contents, decreased by 100%. The decrease in the carbohydrate contents showed a severe degradation of the carbohydrates resulting from fungal decay. Due to the degradation of the lignins, the values of H 1159/H 1508 and H 1058/H 1508, representing the carbohydrate contents, had associated increases of 20% and 48%, respectively.

Tab. 2: The ratio of Fourier-transform infrared spectroscopy characteristic peak height of wood samples.

Decay levels	Samples	The absorption peak height ratio of lignins to carbohydrates			The absorption peak height ratio of carbohydrates to lignins			
		I 1508/I 1159	I 1508/I 1058	I 1731/I 1508	I 1370/I 1508	I 1159/I 1508	I 1058/I 1508	I 897/I 1508
	Control	1.68	2.82	0.37	0.29	0.60	0.35	0.21
Level 1 (severe decay)	No. 1, 2, 3, 5, and 6	1.40	1.91	0.00	0.00	0.71	0.52	0.00
	Change amount	-16%	-32%	-100%	-100%	20%	48%	-100%
Level 2 (moderate decay)	No. 4, 9, and 11	1.31	2.92	0.00	0.37	0.76	0.34	0.00
	Change amount	-22%	4%	-100%	27%	28%	-4%	-100%
Level 3	No. 7 and	1.69	2.90	0.00	0.26	0.59	0.34	0.00

(mild decay)	10							
	Change amount	1%	3%	-100%	-10%	-1%	-3%	-100%
Note: + - increase percentage, − - decrease percentage.								

In samples No. 4, 8, and 9, the value of H 1508/H 1159 had a 22% reduction, showing a degradation of the lignins resulting from fungal decay; the values of H 1731/H 1508 and H 897/H 1508 decreased by 100%, which indicated the severe degradation of the carbohydrates resulting from fungal decay. Due to the degradation of the lignins, the values of H 1370/H 1508 and H 1159/H 1508 had associated increases of 27% and 28%, respectively (Tab. 2).
In samples No. 7 and 10, the value of H 1508/H 1159 and H 1508/H 1058 did not have a noticeable reduction; however, the values of H 1731/H 1508 and H 897/H 1508 decreased by 100%, which indicated the severe degradation of the carbohydrates resulting from fungal decay (Tab. 2).

Discussion

Abundant precipitation in Chikan town makes the relative humidity of the environment too large. The warm and rainy weather also created suitable conditions for the growth of decaying fungi. As a rule, brown-rot fungi can mainly attack both cellulose and hemicellulose but retain lignins of half wet soft woods; while white-rot fungi can consume cellulose, hemicellulose, and lignin of half wet hard woods, especially for the degradation of lignin fast; and soft-rot fungi can mainly attack cellulose, hemicellulose and lignin of both wet soft woods and hard woods in long-term contact with water or in moist soil, especially for the degradation of cellulose fast (Guo et al. 2010). According to the degradation results of the three major chemical compositions with polarized light, fluorescence and FTIR spectra, it was determined that these samples were damaged by soft-rot fungi, and the decay extent of samples No. 1, 2, 3, 5, and 6 were the most serious and were classified as Level I (severe decay), followed by samples No. 4, 8, and 9 and were classified as Level II (moderate decay), with samples No. 7 and 10 having the least decay and were classified as Level III (mild decay).

CONCLUSIONS

The extent of decay in samples No. 1 through 10 from the wood components of arcade buildings in the ancient town Chikan was determined via bright-field light, polarized light, fluorescence, and FTIR spectra. The conclusions are as follows: *(1)* In samples No. 1, 2, 3, 5, and 6, not only the total birefringence brightness but also the green fluorescence brightness was considerably reduced. The absorption peaks representing carbohydrates and lignin disappeared or considerably decreased, indicating that both the carbohydrates and lignins were degraded by decay fungi. Samples No. 1, 2, 3, 5, and 6 were classified as Level I (severe decay). *(2)* In samples No. 4, 8, and 9, the total brightness of birefringence and green fluorescence was also considerably reduced. The extent of decline of absorption peaks representing carbohydrates and lignin was less than that of the first group. Samples No. 4, 8, and 9 were classified as Level II (moderate decay). *(3)* In samples No. 7, and 10, the total brightness of birefringence and green

fluorescence was consistent with those of the control. Compared with the first two groups, the absorption peak intensity of the third group decreased the least. Samples No. 7 and 10 were classified as Level III (mild decay).

ACKNOWLEDGMENTS

The authors gratefully acknowledge the financial support from the Cross-science Research Project of Nanyang Institute of Technology (230068), the Scientific Research Start-up Projects of Nanyang Institute of Technology (510144) and the Science and Technology Project of Henan Province (212102310225).

REFERENCES

1 Arias, M.E., Rodríguez, J., Pérez, M.I., Hernández, M., Polvillo, O., González-Pérez, J.A., González-Vila, F.J., 2010: Analysis of chemical changes in *Picea abies* wood decayed by different *Streptomyces* strains showing evidence for biopulping procedures. Wood Science and Technology 44(2): 179-188.

2 Bari, E., Daniel, G., Yilgor, N., Kim, J.S., Tajick-Ghanbary, M.A., Singh, A.P., Ribera, J., 2020: Comparison of the decay behavior of two white-rot fungi in relation to wood type and exposure conditions. Microorganisms 8(12): 1-20.

3 Bari, E., Daryaei, M.G., Karim, M., Bahmani, M., Schmidt, O., Woodward, S., Ghanbary, M.A.T., Sistani, A., 2019: Decay of *Carpinus betulus* wood by *Trametes versicolor*. An anatomical and chemical study. International Biodeterioration and Biodegradation 137: 68-77.

4 Brischke, C., Stricker, S., Meyer-Veltrup, L., Emmerich, L., 2019: Changes in sorption and electrical properties of wood caused by fungal decay. Holzforschung 73(5): 445-455.

5 Chang, L., Rong, B., Xu, G., Meng, Q., Wang, L., 2019: Mechanical properties, components and decay resistance of *Populus davidiana* bioincised by *Coriolus versicolor*. Journal of Forestry Research 31: 2023-2029.

6 Cheng, J.Q., Yang, J.J., Liu, P., 1992: Chinese timber records. Pp 86-88, China Forestry Publishing House, Beijing.

7 Choi, J.W., Choi, D.H., Ahn, S.H., Lee, S.S., Kim, M.K., Meier, D., Faix, O., Scott, G.M., 2006: Characterization of trembling aspen wood (*Populus tremuloides* L.) degraded with the white rot fungus *Ceriporiopsis subvermispora* and MWLs isolated thereof. Holz als Roh- und Werkstoff 64(5): 415-422.

8 Croitoru, C., Spirchez, C., Lunguleasa, A., Cristea, D., Roata, I.C., Pop, M.A., Bedo, T., Stanciu, E.M., Pascu, A., 2018: Surface properties of thermally treated composite wood panels. Applied Surface Science 438: 114-126.

9 Cui, H., Yang, S., Liu, X., Ma, J., Tian, G., 2016a: Chemical composition and lignin distribution of *Salix integra*. Chemistry and Industry of Forest Products 36(5): 120-126.

10 Cui, X., Qiu, J., Gao, J.R., 2016b: Evaluation of the decay level and reinforcement of ancient wood by fluorescence and polarizing technology. Sciences of Conservation and Archaeology 28(4): 48-53.
11 Dong, S., Wang, C., Xiang, J., Zhang, G., 2020: Research on changes of chemical composition and structure of the minor carpentry work in Gongshu Hall of Hu county based on FTIR-ATR. Infrared 41(7): 30-37.
12 Fahey, L.M., Nieuwoudt, M.K., Harris, P.J., 2019: Predicting the cell-wall compositions of solid *Pinus radiata* (radiata pine) wood using NIR and ATR FTIR spectroscopies. Cellulose 26(13-14): 7695-7716.
13 Ferraz, A., Durán, N., 1995: Lignin degradation during softwood decaying by the ascomycete *Chrysonilia sitophila*. Biodegradation 6(4): 265-274.
14 Gao, S., Yue, X., Wang, L., 2019: Effect of the degree of decay on the electrical resistance of wood degraded by brown-rot fungi. Canadian Journal of Forest Research 49(2): 145-153.
15 Girometta, C., Dondi, D., Baiguera, R.M., Bracco, F., Branciforti, D.S., Buratti, S., Lazzaroni, S., Savino, E., 2020: Characterization of mycelia from wood-decay species by TGA and IR spectroscopy. Cellulose 27: 6133-6148.
16 Guo, M.L., Lan, H.F., Qiu, J., 2010: Wood deterioration and preservation. Pp 161-168, China Metrology Publishing House, Beijing, China.
17 Highley, T.L., Murmanis, L.L., 1987: Micromorphology of degradation in western hemlock and sweetgum by the white-rot fungus *Coriolus versicolor*. Holzforchung 41(2): 67-71.
18 Ibrahim, M.N.M., Yusof, N.N.M., Hashim, A., 2007: Comparison studies on soda lignin and soda anthraquinone lignin. Malaysian Journal of Analytical Sciences 11(1): 206-212.
19 Kanbayashi, T., Miyafuji, H., 2016: Effect of ionic liquid treatment on the ultrastructural and topochemical features of compression wood in Japanese cedar (*Cryptomeria japonica*). Scientific Reports 6: 1-8.
20 Kiyoto, S., Yoshinaga, A., Fernandez-Tendero, E., Day, A., Chabbert, B., Takabe, K., 2018: Distribution of lignin, hemicellulose, and arabinogalactan protein in hemp phloem fibers. Microscopical Society of Canada 24(4): 442-452.
21 Li, G., Huang, A., Qin, T., Huang, L., 2010: FTIR studies of Masson pine wood decayed by brown-rot fungi. Spectroscopy and Spectral Analysis 30(8): 2133-2136.
22 Li, S., Gao, Y., Brunetti, M., Macchioni, N., Nocetti, M., Palanti, S., 2019: Mechanical and physical properties of *Cunninghamia lanceolata* wood decayed by brown rot. Forest 12(3): 317-322.
23 Liu, C., Su, M., Zhou, X., Zhao, R., Lu, J., Wang, Y., 2017a: Analysis of content and distribution of lignin in cell wall of transgenic poplar with Fourier infrared spectrum (FTIR) and confocal laser scanning microscopy (CLSM). Spectroscopy and Spectral Analysis 37(11): 3404-3408.
24 Liu, X., Jin, K., Cui, H., Ma, J., 2017b: The lignin topochemistry of *Daemonorops margaritae* (Hance) Becc. by molecular spectroscopic imaging. Spectroscopy and Spectral Analysis 37(10): 3138-3144.

25 Ma, J., Ji, Z., Zhou, X., Zhang, Z., Xu, F., 2013: Transmission electron microscopy, fluorescence microscopy, and confocal Raman microscopic analysis of ultrastructural and compositional heterogeneity of *Cornus alba* L. wood cell wall. Microscopy and Microanalysis 19(1): 243-253.
26 Monrroy, M., Ortega, I., Ramirez, M., Baeza, J., Freer, J., 2011: Structural change in wood by brown rot fungi and effect on enzymatic hydrolysis. Enzyme and Microbial Technology 49(5): 472-477.
27 Pandey, K.K., Nagveni, H.C., 2009: Rapid characterisation of brown and white rot degraded chir pine and rubberwood by FTIR spectroscopy. Holz als Roh- und Werkstoff 65(6): 477-481.
28 Pandey, K.K., Pitman, A.J., 2003: FTIR studies of the changes in wood chemistry following decay by brown-rot and white-rot fungi. International Biodeterioration & Biodegradation 52(3): 151-160.
29 Stark, N.M., Matuana, L.M., 2004: Surface chemistry changes of weathered HDPE/wood-flour composites studied by XPS and FTIR spectroscopy. Polymer Degradation and Stability 86(1): 1-9.
30 Stark, N.M., Matuana, L.M., 2007: Characterization of weathered wood-plastic composite surfaces using FTIR spectroscopy, contact angle, and XPS. Polymer Degradation and Stability 92(10): 1883-1890.
31 Tamburini, D., Łucejko, J.J., Pizzo, B., Mohammed, M.Y., Sloggett, R., Colombini, M.P., 2017: A critical evaluation of the degradation state of dry archaeological wood from Egypt by SEM, ATR-FTIR, wet chemical analysis and Py(HMDS)-GC-MS. Polymer Degradation and Stability 146: 140-154.
32 Tomak, E. D., Topaloglu, E., Gumuskaya, E., Yildiz, U.C., Ay, N., 2013: An FTIR study of the changes in chemical composition of bamboo degraded by brown-rot fungi. International Biodeterioration and Biodegradation 85: 131-138.
33 Wentzel, M., Rolleri, A., Pesenti, H., Militz, H., 2019: Chemical analysis and cellulose crystallinity of thermally modified *Eucalyptus nitens* wood from open and closed reactor systems using FTIR and X-ray crystallography. European Journal of Wood and Wood Products 77(4): 517-525.
34 Xu, G., Wang, L., Liu, J., Wu, J., 2013: FTIR and XPS analysis of the changes in bamboo chemical structure decayed by white-rot and brown-rot fungi. Applied Surface Science 280: 799-805.
35 Yang, Y., He, Y., Han, L., Wang, A., Wang, W., Zhao, R., Li, B., 2020b: Application of histochemical stains for rapid qualitative analysis of the lignin content in multiple wood species. BioResources 15(2): 3524-3533.
36 Yang, Y., Sun, H., Li, B., Han, L., Wang, A., Wang, W., He, Y., Zhao, R., 2020a: Study on the identification and the extent of decay of the wooden components in the Xichuan Guild Hall ancient architectures. Pp 1-10, International Journal of Architectural Heritage.

37 Yang, Y., Sun, H., Li, B., Wang, A., Zhao, R., Wang, W., He, Y., Yang, S., Han, Y., Sun, W., 2020c: Fourier-transform infrared spectroscopy analysis of the changes in the chemical composition of wooden components in the ancient building of Xichuan Guild Hall. Forest Products Journal 70(4): 448-452.
38 Yang, Y., Sun, H., Yang, S., Sun, W.Y., Zhao, Y., Li, B., Wang, W., Zhang, X.Q., Jiang, S.L., Xu, Q., 2021b: Fourier-transform infrared spectroscopy analysis of the changes in chemical composition of wooden components: Part II. The ancient building of Danxia temple. Forest Products Journal 71(3): 283–289.
39 Yang, Y., Sun, H. Yang, S., Wang, A.F., Zhao, R., Wang, W., He, Y.M., Li, B., Zhang, B.X., Wu, Q., 2021a: Internal cause analysis of damage of wooden components in Danxia temple ancient Architectures: tree species. Wood Research 66(2): 297-308.
40 Yang, Y., Zhan, T.Y., Lu, J.X., Jiang, J.H., 2015: Influences of thermo-vacuum treatment on colors and chemical compositions of alder birch wood. BioResources 10(4): 7936-7945.
41 Zeng, Y., Yang, X., Yu, H., Zhang, X., Ma, F., 2012: The delignification effects of white-rot fungal pretreatment on thermal characteristics of Moso bamboo. Bioresource Technology 114: 437-442.

YAN YANG*, XIAOQIAN ZHANG, QIAN XU, PEIYANG WANG, SHILONG JIANG,
YAN MIN, WENYE SUN, BIN LI, YULONG FAN
NANYANG INSTITUTE OF TECHNOLOGY
SCHOOL OF ARCHITECTURE
CHANGJIANG ROAD 80#, WANCHENG DISTRICT
NANYANG CITY, HENAN PROVINCE
CHINA
*Corresponding author: yangyanrainy@163.com

SHUANG YANG
HENAN UNIVERSITY MINSHENG COLLEGE
SCHOOL OF ECONOMICS
JINMIN STREET, LONGTING DISTRICT
KAIFENG CITY, HENAN PROVINCE
CHINA